Spring 2022

Location and Calibration of Lightning Pulses from LOFAR Radiation Measurements

Nicholas R. Demers
University of New Hampshire, Durham

Location and Calibration of Lightning Pulses from LOFAR Radiation Measurements

N. Demers*

University of New Hampshire, Durham, NH, 03824, USA

(Dated: May 27, 2022)

Lightning has the power to shock and awe as an incredible force of nature, yet so many phenomena surrounding lightning are still not well-understood. In fact, the very physics regarding what actually sparks a lightning strike remain poorly defined. In an effort to understand how lightning initiation is achieved, data collected from the Low Frequency Array in the Netherlands were calibrated and interferometry performed to map the flash in 4D space. The calibration process itself is explored, from choosing lightning sources to calibrate, to the various stages of calibration leading to a fully calibrated flash ready for interferometric analysis. Using these calibrations, other researchers will be able to explore initiation and other lightning phenomena.

INTRODUCTION

Lightning is a common occurrence which any given person has seen or interacted with in their life. Lightning is immortalized through classical Greek mythology, in such works as Mary Shelley's novel *Frankenstein*, and has been an object of fascination since the beginning of history. From the Greek Zeus to the Japanese Raijin to the Nordic Thor, humans have always sought to explain this incredible natural phenomenon. In modern times we know lightning to be mere electrical discharge of a massive caliber instead of a flexing of divine might, but the desire to better understand it persists. While the modern study of lightning is often attributed to Benjamin Franklin in the mid 1700s, incredible discoveries about the fundamental nature of lightning have been made as recently as the late 1900s with the discovery and documentation of previously unknown types of lightning.[1] Such ongoing discoveries demonstrate the great wealth of knowledge still yet to be uncovered.

One such mystery revolves around the mechanism for triggering lightning. The general characteristics of a thundercloud and the environment within such a cloud at the time of lightning initiation are fairly well-studied,

but the actual initiation phenomenon which triggers a flash remain undiscovered. Discovering and understanding this initiation mechanism would be a huge step in lightning research, and could provide a key to other fundamental questions around lightning physics.

The first step along this road, of course, is to create high-resolution images of lightning and the radiation environment before, during, and after a lightning flash. Thus, calibration of radiation data is necessary. By carefully calibrating and imaging flashes, aspects of lightning can be analyzed in better detail than ever before and hopefully result in electrifying new discoveries.

What is Lightning

In order to adequately characterize and discuss lightning, a few basic definitions are necessary. The Oxford English Dictionary defines lightning as *"A flash, or several flashes, of very bright light in the sky caused by electricity"*.[2] Lightning researchers modify this definition little, calling lightning *"a transient, high-current electric discharge whose path length is measured in kilometers"*.[3] Lightning comes in many varieties, including the well-known cloud-to-ground, inter-cloud, and intra-cloud lightnings, but also the more recent discoveries of Transient Luminous Events (TLE's) which include types of lightning such as red sprites, halos, blue starters, blue jets, gigantic jets, and elves.[4] Collectively, lightning is grouped into two basic categories: flashes which bridge the gap between the cloud and Earth, and flashes which don't bridge that gap. The first category contains cloud-to-ground flash types, whereas the second contains inter/intra-cloud flashes and TLE's. Cloud-to-ground lightning, being the most studied form of lightning due to its easily observable nature and direct impact to humans, is used in the following paragraph to define the time evolution of a lightning flash.

Lightning flashes are broken into basic components called strokes, of which a typical strike has 3 to 5, and have been observed to have anywhere from 1 to 26. Each stroke is further broken down into two parts: the leader and the return stroke, which always occur in that order. Following lightning initiation, an initial negative leader is formed which creates a conducting path from the initiation point to the ground. This path allows for charge to be distributed from the cloud to the ground. Initial negative leaders are also called 'stepped leaders' due to the intermittent nature of their propagation as they forge the path between the cloud and ground. Following the initial leader, the return stroke follows the same path as the leader, but in the opposite direction, neutralizing the charge
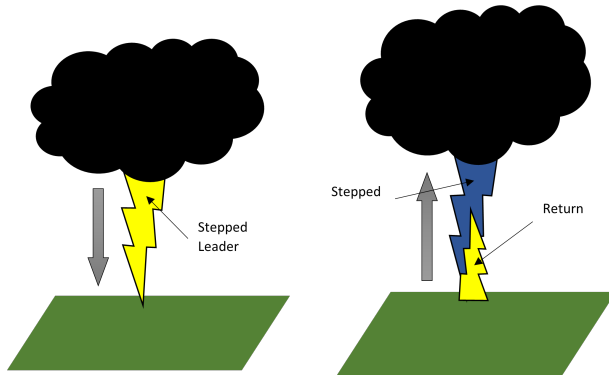
Figure 1: Time evolution of cloud-to-ground lightning strike illustrating the initial, or stepped, leader and the following return stroke.

from the leader. This basic time evolution is shown in Fig. 1

Subsequent leaders travel along the same path as the stepped leader, and as a result don't share the same intermittent nature. These subsequent leaders are also called 'dart leaders'.[5]

What is LOFAR

The Low-Frequency Array, or LOFAR, is described as a new-generation radio interferometer, and is a series of antennas centered in the Netherlands and spread throughout Europe. The full system consists of about 20,000 antennas grouped into 52 stations, 38 of which are in the Netherlands. The other 14 stations are located in Germany, Poland, France, Great Britain, Ireland, Latvia, and Sweden.

LOFAR is unique in that it was designed to take readings in a low-frequency domain spanning 10-240 MHz with the expectation of use for various pulsar, solar, cosmic ray, and extra-galactic research. However, it was discovered that the data gathered by LOFAR was excellent for lightning research as well, clouds being invisible in this range.

For the flash analyzed here, only Netherlands based LOFAR antennas were used. These antennas are broken down into stations, which are further subdivided into core stations (CS) shown in Fig. 2 and remote stations (RS) shown in Fig. 3. Core stations are stations which are located in close proximity to the LOFAR collection node, whereas remote stations are up to 90 kilometers away. For data collection, clocks are connected to each station. Core stations all operate on one clock connected by fibre-optic cabling, whereas each remote station has its own GPS clock.

A single stations consists of 96 low-band antennas (LBA's) grouped into two circles, and 48 high-band antennas (HBA's) optimized for 30-80 MHz and 120-240 MHz respectively. LBA's are simple antennas, operating in collocated and orthogonal pairs to resolve two polarizations. One polarization is oriented northwest-southeast and the other northeast-southwest. HBA's are organized into tiles, with core stations having two tiles
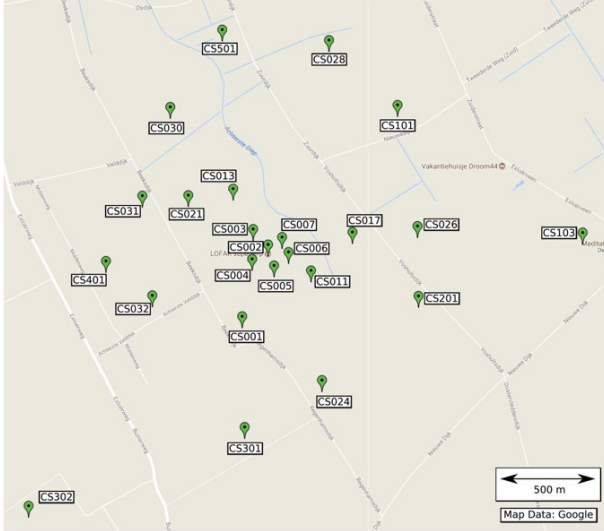
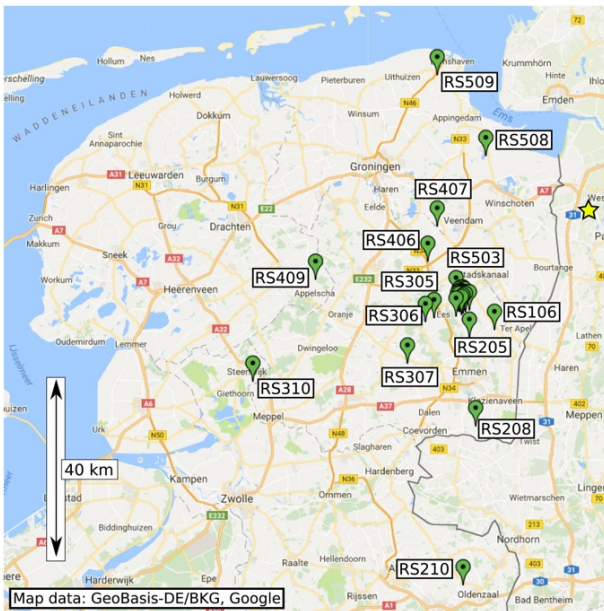Figure 2: LOFAR core stations located in the Netherlands[6]

Figure 3: LOFAR remote stations located in the Netherlands. Core stations visible as a cluster of green pins near RS205[6]

of 24 HBA's, and remote stations having one. For this research, only data from six pairs of LBA's are used per station to keep data size manageable.

Additionally, data collection is limited by the digitization of the signals recorded by the station antennas. Each station has 48, three-input digital receiver units (RCU's) to collect the data from the antennas via coaxial cabling. Two of these inputs are dedicated to LBA's, and the remaining one to HBA's. However, only one input can be active at a time, resulting in a maximum of either half the LBA's or all of the HBA's being processed at once. Up to 5 seconds of data, in the form of radiation amplitude vs time as shown in Fig. 6, can be stored locally at the stations in the RCU's. Then, upon receiving a dump command, the station pauses collection to read this data out. Per antenna, it takes 30 seconds to relay 1 second of data, so reading out 5 seconds from 6 pairs of antennae takes 30 minutes. This means that for every 5 seconds of data read out, the following 30 minutes are lost.

The data is then sent to a collection node using a wide-area network (WAN). The LOFAR WAN uses light-paths which route data from stations to the collection node within the core stations, and thence to the University of Groningen for final storage, processing, and dissemination.[7][8][6]

Interferometry

Interferometry in this context refers to the process of locating lightning pulses in 4D space: three spatial dimensions and one time dimension. To do so accurately requires that very few approximations are made, but this process is not done manually, and for illustrative purposes we can assume antennas are co-planar, that times are exact, and that the source emits a plane-wave.

To position lightning in 4D space, between 150 and 200 antennas from 29 stations are used, (the exact number varies per flash) but in order to understand the general idea, one can consider the case of locating a source in 2D space using three antennas, as shown in Fig. 4.
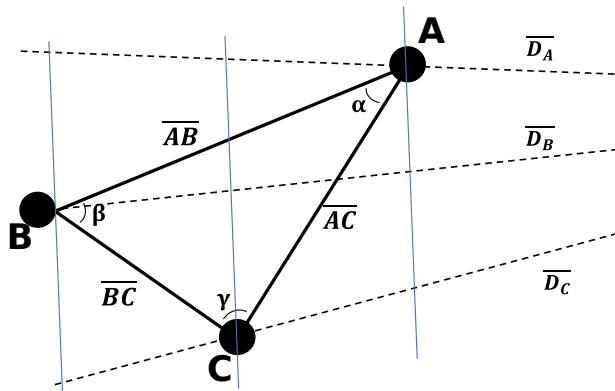

Figure 4: Basic 2D interferometry problem with 3 antennas. Positions of antennas **A**, **B**, and **C** are known, as is the time at which each antenna received the signal.

We know the time the signal arrived at each station, commonly denoted as τ_A, τ_B, and τ_C, as well as the coordinates of each antenna, so the lengths of $\overline{AB}$, $\overline{AC}$, and $\overline{BC}$ are known, as are the angles α, β, and γ. We can guess the relative quadrant in which the source lies by comparing the time at which each antenna receives the signal. In this case, antenna **A** receives the signal first, followed by **C**, then **B**, indicating the general location of the pulse to be in quadrant one. Lines $\overline{D_A}$, $\overline{D_B}$, and $\overline{D_C}$ can be drawn from each antenna to an arbitrary guess position in the correct quadrant to provide a basis for further computations. Lines imitating the plane-wave at each antenna, shown in blue in Fig. 4, can then be drawn from the antennas to a close, but not quite perpendicular, intersection with $\overline{D_B}$. These imitation lines serve to illustrate the propagation of the source at our guess location. $\overline{D_A}$ and $\overline{D_C}$ can then be extended to intersect with the plane-wave at antenna **B** to complete our picture. These lines create a complex series of triangles which can be solved for using various trigonometric functions and identities. A refresher of these equations is given in Table I.

Once these triangles are solved, and knowing that the relation between time and distance is given by $distance = c * time$, the correct line equation can be applied to the initial guess lines. The point at which the

Function	Equation
Sine	$\sin \alpha = \frac{opposite}{hypotenuse}$
Cosine	$\cos \alpha = \frac{adjacent}{hypotenuse}$
Tangent	$\tan \alpha = \frac{opposite}{adjacent}$
Law of Sines	$\frac{\sin \alpha}{|A|} = \frac{\sin \beta}{|B|} = \frac{\sin \gamma}{|C|}$
Law of Cosines	$|C| = \sqrt{A^2 + B^2 - 2|A||B|\cos(\angle \overline{AB})}$

Table I: Basic trigonometric functions and
identities useful to the performance of
interferometry.

three intersect is then the absolute location
of the source.

Stage	Description
1: Explore Run	Initial search through raw data to discover possible source locations
2: Station Calibration	Rough alignment on the level of entire stations
3: Antenna Calibration	Fine alignment of individual antennas within each station
4: Imaging	Generation of plots showing the structure of the flash in 4D space, as well as plots showing the magnitude of individual pulses compared to background radiation

Table II: Overview of calibration steps for
any given lightning flash.

CALIBRATION

In order to perform interferometry and get a clear image of a flash, the data from LO-FAR must first be calibrated. Each core station operates from a single GPS clock which connects to the stations through fibre-optic cabling. This cabling is only accurate to about 10 nanoseconds, though, and introduces slight timing offsets amongst the core stations. The remote stations each have their own GPS clock, each of which can be off from the others, so timing offsets can be as large as hundreds of nanoseconds. Using previous calibrations from flashes chronologically nearby can greatly assist the calibration process, but both the cabling offsets and GPS clock offsets are unknown and ever-changing. A single lightning pulse has been observed to last between 100-2000 nanoseconds, so to study structure and initiation phenomena, these offsets must all be discovered and corrected for with each flash.[6]

A general outline of the steps required is given in Table II

Explore Run

The first step in this process is to initiate an explore run. An explore run sifts through

the LOFAR data from high-activity times during thunderstorms to find time chunks where the signal received by the antenna is significant compared to the galactic background which comprises the majority of the noise within the signal. These times are analyzed interferometrically to obtain an initial guess regarding the location of each potential chunk. Upon completion, a graph and data table are both generated containing the chunk ID, location guess in 4D space, and the chi^2 value corresponding to how well these guessed locations fit the chunks. For lightning flash 21C-6, a sample of this data table is shown in Table III.

Chunk ID	Time (ms)	Northing (km)	Easting (km)	Height (km)	Chi^2
101	238.	-12.536931	11.270592	5.1646740	1.185667
1507	658.	1.9145999	4.7213032	7.3953532	19.018434
1817	748.	2.4689943	5.4728607	11.373085	0.608354
2101	838.	2.0062325	0.20072048	5.5912157	0.938125
2538	958.	-10.901852	10.264120	10.839819	0.510463
3334	1198.	7.7793030	2.074585	14.123211	1.641370
3735	1318.	-6.1270268	11.642714	4.9006572	23.903887
4322	1498.	-9.9265110	0.52443252	9.1235721	16.961321

Table III: A selection of explore run chunks from the 21C-6 flash. Total data table output contained 1105 data points.

Also generated is a representation of these chunks in the 4D domain, shown in Fig. 5. While certainly unrecognizable as lightning, this image gives lots of detail about the possible shape and timing of the flash. The top panel showing height vs time is rather self-explanatory, but the bottom panel is less intuitive. The 'Northing' scale represents the chunks' relative north/south location, and the 'Easting' scale represents the relative east/west location. Therefore, the bottom left graph shows a top-down view of the chunks, and the two other graphs show cuts of cardinal direction and height, with all points color coded by time as defined in the time legend.

Sorting the explore run data table by increasing chi^2, up to 6 chunks can be used for calibration. For the 21C-6 flash, 4 were chosen. A few points bear noting when defining the initial chunks. First, the locations of the chunks provided by the explore run are very rough. The resultant data table contains 8 significant figures for spatial positioning, but the accuracy of these guesses is poor enough that rounding the values to the nearest hundred, or even thousand meters makes no difference. Also, any given chunk spans 0.3 ms. Knowing this, the initial calibration script can be run iteratively over the span of multiple milliseconds with a 0.3 ms step to find a more precise time for each chunk. By round-
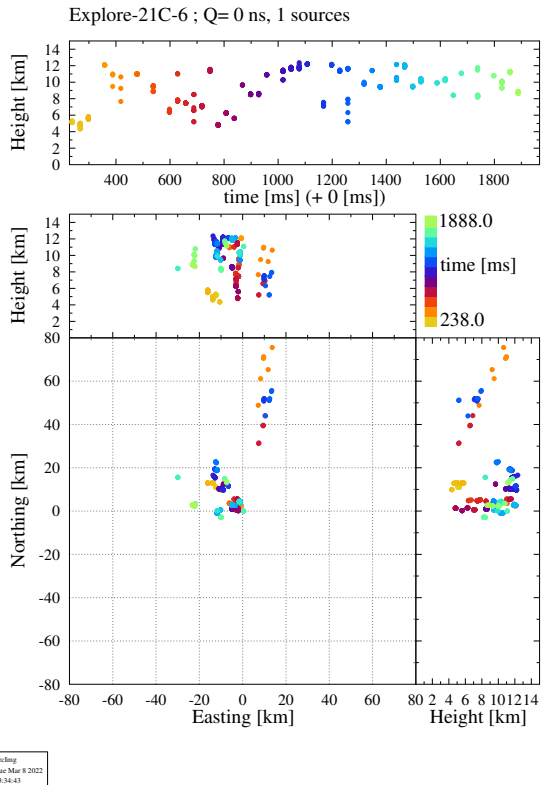
Figure 5: Explore run output for lightning flash 21C-6 represented in 4D space.

Time (ms)	Northing (m)	Easting (m)	Height (m)
356.2	-6100	3500	11000
478.4	-6100	3500	11000
1196.8	-6600	11500	12000
1738.0	-9999	-2900	8300

Table IV: Selected chunks for use in calibrating lightning flash 21C-6, with locations generalized and times optimized.

When running the calibration script on the chunks selected from the explore run, there are three main outputs to look at: the overall chi^2 value, CuP files, and updated pulse data.

The overall chi^2 value at this point is given as two values, one for each antenna polarity. These values provide an at-a-glance indicator of the goodness of fit for the flash, and signals readiness to proceed to the next stage when they get 'low enough'. Conditions for what constitutes 'low enough' will be discussed further on.

The updated pulse data are a table of individual lightning pulses within each chunk that contain various pieces of information about the pulse. An example of one pulse is shown in Table V.

ing the spatial coordinates and more precisely locating the temporal coordinate, script input is optimized and calibration can proceed to the next stage. Following this rounding and pinpointing procedure, the values in Table IV were used as initial input.

Stage 1: Station Calibration

The first stage of alignment is to do a rough calibration of the stations as a whole.

Number	Polarity	Chunk	Sample Offset
1	0	1	4931

Nothing	Easting	Height	Reference Time	Chi^2
2287.04	-728.88	11884.15	356.40647	0.95

Table V: Data from a single pulse update given in the output of the calibration script, including pulse ID number, polarity value, chunk number, sample number at the peak of the time trace, 3D spatial coordinates, the time recorded at a reference station, and the goodness of fit chi^2 value.

Each chunk contains multiple pulses with corresponding even and odd polarities, so the output assigns each pulse an arbitrary identification number as the first value. The second number specifies the polarity of the signal, (either 1 for odd or 0 for even) the third number states the chunk it's contained within, and the fourth is the offset from the beginning of the chunk specifying where the peak of the pulse is on the time trace. Following those, a new spatial coordinate guess is given, then the time in ms at the reference station, and finally the chi^2 of the pulse. At this point, improving the calibration is contingent upon improving the fit at the individual pulse level, so this table of new pulse data is incredibly important. By iteratively running the script and updating the input file with the new pulse data generated by each run, the overall chi^2 value can be much reduced. However, this method of iterative calibration only goes so far, and eventually the overall chi^2 will plateau. Once that plateau has been reached, the third output is used to continue improving the fit.

CuP images are generated for each even polarity pulse, and contain the time trace of the pulse across all stations for both the even polarity and the corresponding odd polarity. The position of the pulse in time is defined by the 4D guess parameters used in the input file, and the better the alignment of the traces within a pulse, the better the calibration has found the timing offsets. A portion of a CuP file from 21C-6 is shown in Fig. 6. This image shows nine of the CS time traces which have been well aligned. For each station there are two traces: the even polarity on the horizontal line, and the odd polarity above the line, with antennas for each overlaid atop each other. However, while the stations are well aligned, it's apparent that the individual antennas of CS001 and CS028 are not, as evidenced by the fact that they're noticeably more offset from each other.

To decrease the overall chi^2, CuP files are visually inspected and any stations which are not well aligned are excluded from the
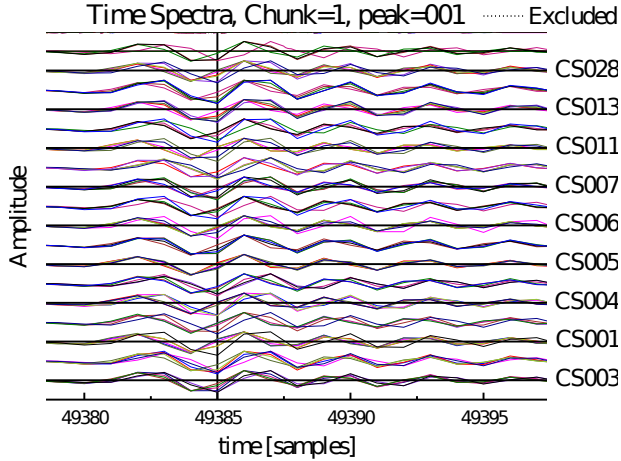
Figure 6: A portion of a CuP showing the time trace of pulse 1 for nine core stations. Even polarity traces are on a line, and odd polarity traces are shown just above the line. Antennas from each station/polarity are superimposed upon each other.

fit. Due to the relatively small timing offsets within the core stations, a typical CuP file will initially have a structure where the core stations are mostly well aligned and the remote stations are very poorly aligned. By excluding stations which appear most offset, and having the calibration script ignore these stations during fitting, the script is usually able to provide better fit parameters and locations. A simple method of excluding stations is to begin by treating both polarities together and excluding all of the remote stations. Then, running the fit code, updating the pulse data, and repeating this process while adding in the remote stations one by one will gradually improve the fit. Any

station that causes the chi^2 to drastically increase or the CuP file to become noticeably worse aligned should continue to be excluded. Continuing in this manner should be sufficient to achieve a reasonably low chi^2 across each pulse.

Once all pulses have been treated in this manner and a balance has been found between keeping the individual pulse chi^{2}s low while excluding as few stations as possible, the same steps are repeated again for each pulse. This time, however, the even and odd polarities are treated separately.

After this second round of inspection and exclusion has concluded, the stations should be well aligned and the overall chi^2 values should be no higher than 10, but ideally between 2 and 6. The closer to 1 these values are, the easier the following step will be, and the cleaner the final data will look. An example of a well-aligned pulse for this stage is pulse 006 from flash 21C-6, shown in Fig. 7, and having an even polarity chi^2 of 1.06. This pulse is also ideal in that the area around the pulse has very little noise, and only 3 stations were excluded from the even polarity to achieve this fit.

The final part of stage one calibration is to write a new calibration file containing the corrected station timings. This is done in at least two steps. First, a calibration file is written using the most recent pulse
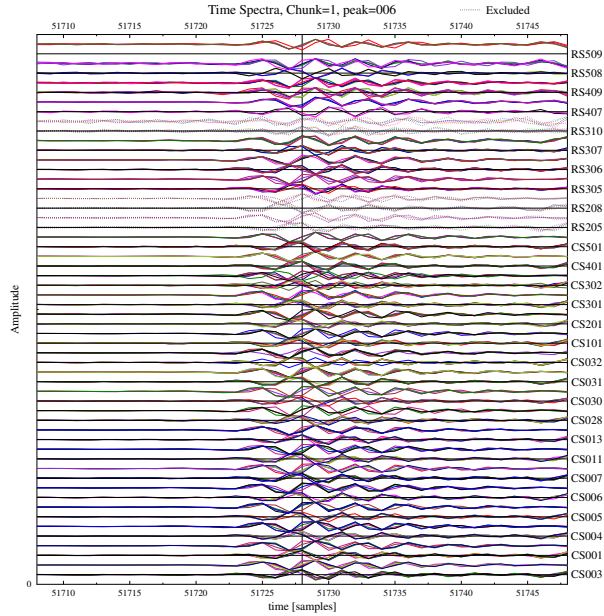
Figure 7: Final alignment of stations for flash 21C-6, pulse 006. Even polarity chi^2 of 1.06 with stations RS205, RS208 and RS310 excluded.

Stage 2: Antenna Calibration

The second stage of alignment is to calibrate the individual antennas within each station. This stage is remarkably similar to the execution of the station calibration stage, but differs significantly in approach. When fitting antennas, a new calibration file should be written with each run of the calibration script, and the most recently generated calibration file should be used at all times. The one exception to this is in the case of a run in which the alignment of antennas is found to be worsened upon visual inspection. If this is the case, the previous calibration file should be kept until a better one is written.

To actually fit the antennas, a method similar to the final step of station calibration is used. In the calibration input file up to 6 stations can be specified at a time, and the antennas for each of these stations will be calibrated and a new calibration file written for those corrections. The easiest approach is to again start with the core stations and work outward to the remote stations. Ideally, each station's antennas should only need to be fit once to achieve a good calibration. However, this isn't always the case, and for some flashes it's necessary to run various combinations of stations at once in order to properly align the antennas. An example of the effect of fitting antennas is shown in Fig. 8, taken from pulse

locations but only fitting the core stations. Previously, a default calibration file was used as the base for the fit code, but the newly made calibration file is now substituted in. After setting the fit code to use the new calibration file, pulse locations are updated again and then another new calibration file is written, only fitting the remote stations. This calibration file is the final product for the station fitting stage, and should result in well-calibrated CuP files being generated.

006, which shows the antennas from station RS306 before and after calibration.

(a) Before fitting antennas
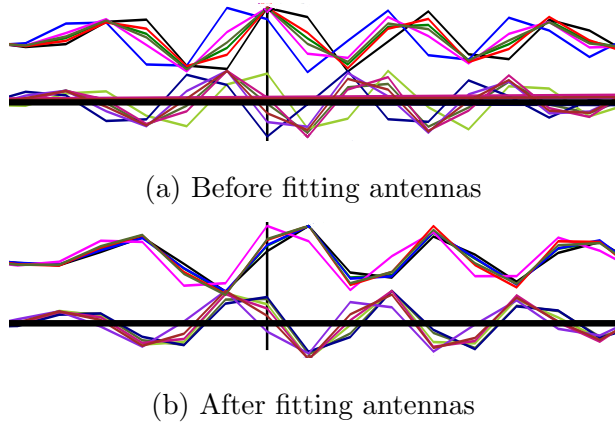

(b) After fitting antennas

Figure 8: Antennas from station RS306, pulse 006, before and after calibration. After fitting, antenna traces noticeably snap together, indicating a good fit.

The traces before fitting are slightly out of phase with each other, but after calibration are almost perfectly aligned.

Another important tool, cross correlation plots, are also generated as output at this stage. Taking the cross correlation of the antennas provides the ability to diagnose antenna specific issues within a particular station. A mostly healthy cross correlation plot, shown in Fig. 9, has smooth, well-aligned curves with maxima centered on the vertical line. In this particular image, the offset of RS208 compared to the other stations is indicative of a poor calibration, but other stations exhibit no such behavior.

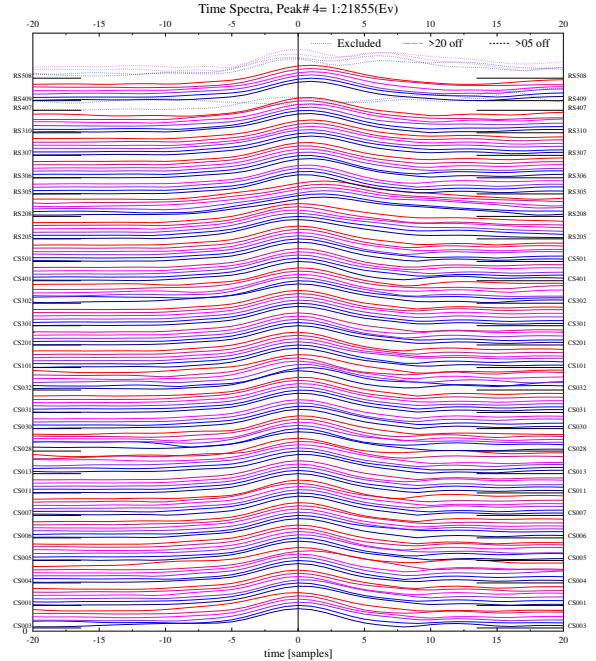There are two common issues which can be

Figure 9: Healthy cross correlation plot from flash 21C-6, pulse 004. Antenna cross correlations, with the exception of RS208, are well aligned and show no signs of phase shifts or polarity flips.

diagnosed using the cross correlation plots: phase shifts, and polarity flips. If a specific antenna appears well-aligned on the CuP images but is actually offset by $2n\pi$, the cross correlation plot will show this as one trace having a peak offset from the others within the station. Polarity flips occur when antennas are flagged as the wrong polarity, and show up in the cross correlation plots as a perfectly mirrored trace. Both of these issues can be corrected for using parameters found in the calibration input file. Once all antennas have been aligned, and any issues

corrected for, the final calibration file can be written and used for analyzing the flash.

RESULTS

With the final calibration file in hand, images of the full flash can be created. These images, like that of flash 21C-6 shown in Fig. 10, show the structure and time evolution of the flash, and can also reveal interesting characteristics. This region is especially active, and further calibration remains to be done to resolve various areas of the flash in higher quality.

Another feature of note within this flash is the possible presence of a novel lightning phenomenon. In the region between northing 13.01 to 13.03, easting -8.89 to -8.87, height 9.76 to 9.81, and spanning a total of 19 ms, an abnormally slow propagation area can be seen. While this could be caused by poor resolution in this region, precedent for finding these events has been established within other flashes.[9]

Originally believed to be a meteor or some other atmospheric anomaly, consultation with astrological groups coupled with the discovery of similar events in other flashes led to thought that this could be a novel phenomenon. The potential presence of this feature is incredibly exciting, but will require more analysis to better resolve the image.
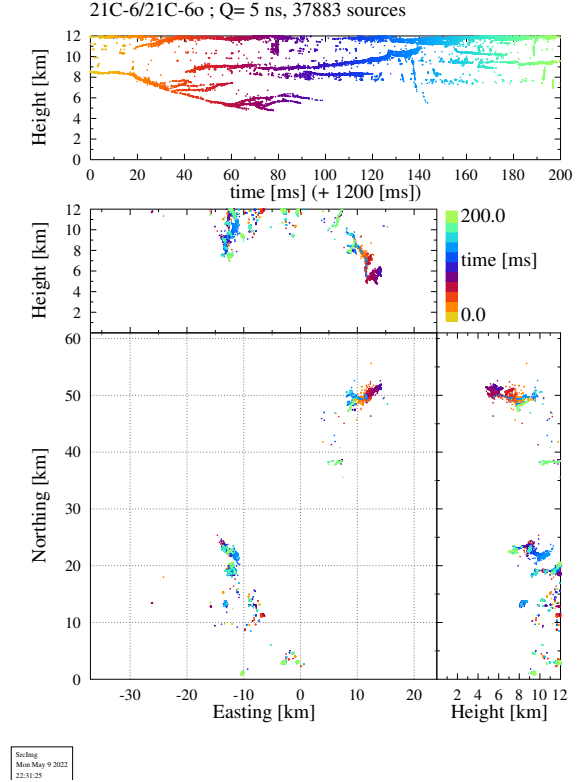

Figure 10: 4D image of flash 21C-6 after calibration. This flash occurred in a high-activity region, and shows potentially interesting areas requiring further calibration.

In addition to the 4D map of the flash, another image which can be created is a beam-formed interferometric image, shown in Fig. 11 for the 20B-10 flash, and focused on the initiation region. The upper portion of Fig. 11 shows what typical radiation measurements would look like; pure noise due to the galactic radio background. Using inter-

feronmetric images made possible by the calibration, however, it's possible to pick out lightning sources from this background and pinpoint them with a precision measurable in meters. As seen in the three panels of Fig. 11 graphing dEast by dNorth, dh by dNorth, and dh by dEast, sources appear as regions of activity much higher than that of the background.

Figure 11: Interferometric image focusing on the initiation region of flash 20B-10

CONCLUSIONS

LOFAR remains a potent tool in burgeoning lightning research, and with ever-improving calibration techniques, high resolution lightning maps and radiation measurements are increasingly easy to generate. With these advancements, answers to questions about lightning initiation draw within reach. By using beam-formed interferometric images as shown previously, researchers can locate the initiation of a flash and then time-step back in tiny increments to analyze activity just before initiation. The hope is that by searching through high-quality radiation data prior to initiation, some feature or process will become apparent as the precursor to initiation.
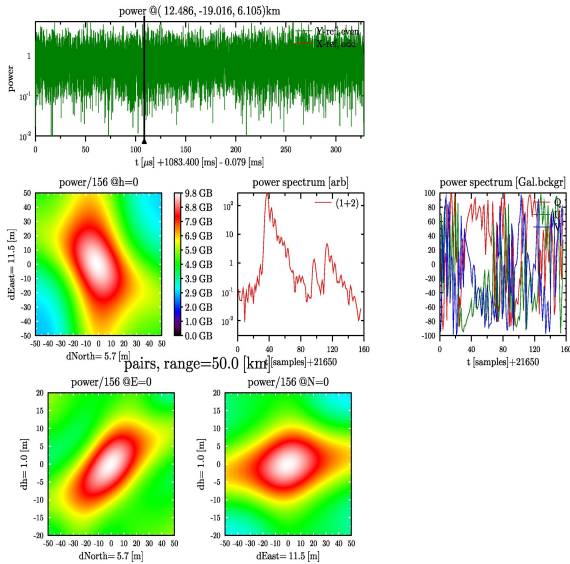
These calibration and imaging techniques have also enabled the discovery of such phenomena as the abnormally slow propagation recently found in various flashes, including our 21C-6 flash. By zooming in on these phenomena and further calibrating the regions around them, it's possible that more lightning secrets will be discovered.

Much work remains to be done, however, and it's our hope that future efforts can focus on automation of the calibration process. Current calibration techniques are equal parts art and science, and involve countless iterations of the same steps. Streamlining and automating this process would allow for a much greater volume of flashes to be analyzed, speeding up research efforts.

ACKNOWLEDGMENTS

---

* Corresponding author: Nicholas.Demers@unh.edu

[1] V. P. Pasko, Journal of Geophysical Research: Space Physics **115**, 0 (2010).

[2] Oxford University Press, lightning.

[3] M. A. Uman, *Lightning* (Courier Corporation, 2012).

[4] J. R. Dwyer and M. A. Uman, Physics Reports **534**, 147 (2014).

[5] V. A. Rakov, Surveys in Geophysics **34**, 701 (2013).

[6] B. M. Hare, O. Scholten, A. Bonardi, S. Buitink, A. Corstanje, U. Ebert, H. Falcke, J. R. Hörandel, H. Leijnse, P. Mitra, K. Mulrey, A. Nelles, J. P. Rachen, L. Rossetto, C. Rutjes, P. Schellart, S. Thoudam, T. N. Trinh, S. ter Veen, and T. Winchen, Journal of Geophysical Research: Atmospheres **123**, 2861 (2018).

[7] M. D. Vos, A. W. Gunst, and R. Nijboer, Proceedings of the IEEE **97**, 1431 (2009).

[8] M. P. V. Haarlem, M. W. Wise, A. W. Gunst, G. Heald, J. P. McKean, J. W. Hessels, A. G. D. Bruyn, R. Nijboer, J. Swinbank, R. Fallows, M. Brentjens, A. Nelles, R. Beck, H. Falcke, R. Fender, J. Hörandel, L. V. Koopmans, G. Mann, G. Miley, H. Röttgering, B. W. Stappers, R. A. Wijers, S. Zaroubi, M. V. D. Akker, A. Alexov, J. Anderson, K. Anderson, A. V. Ardenne, M. Arts, A. Asgekar, I. M. Avruch, F. Batejat, L. Bähren, M. E. Bell, M. R. Bell, I. V. Bemmel, P. Bennema, M. J. Bentum, G. Bernardi, P. Best, L. Bîrzan, A. Bonafede, A. J. Boonstra, R. Braun, J. Bregman, F. Breitling, R. H. V. D. Brink, J. Broderick, P. C. Broekema, W. N. Brouw, M. Brüggen, H. R. Butcher, W. V. Cappellen, B. Ciardi, T. Coenen, J. Conway, A. Coolen, A. Corstanje, S. Damstra, O. Davies, A. T. Deller, R. J. Dettmar, G. V. Diepen, K. Dijkstra, P. Donker, A. Doorduin, J. Dromer,

M. Drost, A. V. Duin, J. Eislöffel, J. V. Enst, C. Ferrari, W. Frieswijk, H. Gankema, M. A. Garrett, F. D. Gasperin, M. Gerbers, E. D. Geus, J. M. Grießmeier, T. Grit, P. Gruppen, J. P. Hamaker, T. Hassall, M. Hoeft, H. A. Holties, A. Horneffer, A. V. D. Horst, A. V. Houwelingen, A. Huijgen, M. Iacobelli, H. Intema, N. Jackson, V. Jelic, A. D. Jong, E. Juette, D. Kant, A. Karastergiou, A. Koers, H. Kollen, V. I. Kondratiev, E. Kooistra, Y. Koopman, A. Koster, M. Kuniyoshi, M. Kramer, G. Kuper, P. Lambropoulos, C. Law, J. V. Leeuwen, J. Lemaitre, M. Loose, P. Maat, G. Macario, S. Markoff, J. Masters, R. A. McFadden, D. McKay-Bukowski, H. Meijering, H. Meulman, M. Mevius, E. Middelberg, R. Millenaar, J. C. Miller-Jones, R. N. Mohan, J. D. Mol, J. Morawietz, R. Morganti, D. D. Mulcahy, E. Mulder, H. Munk, L. Nieuwenhuis, R. V. Nieuwpoort, J. E. Noordam, M. Norden, A. Noutsos, A. R. Offringa, H. Olofsson, A. Omar, E. Orrú, R. Overeem, H. Paas, M. Pandey-Pommier, V. N. Pandey, R. Pizzo, A. Polatidis, D. Rafferty, S. Rawlings, W. Reich, J. P. D. Reijer, J. Reitsma, G. A. Renting, P. Riemers, E. Rol, J. W. Romein, J. Roosjen, M. Ruiter, A. Scaife, K. V. D. Schaaf, B. Scheers, P. Schellart, A. Schoenmakers, G. Schoonderbeek, M. Serylak, A. Shulevski, J. Sluman, O. Smirnov, C. Sobey, H. Spreeuw, M. Steinmetz, C. G. Sterks, H. J. Stiepel, K. Stuurwold, M. Tagger, Y. Tang, C. Tasse, I. Thomas, S. Thoudam, M. C. Toribio, B. V. D. Tol, O. Usov, M. V. Veelen, A. J. V. D. Veen, S. T. Veen, J. P. Verbiest, R. Vermeulen, N. Vermaas, C. Vocks, C. Vogt, M. D. Vos, E. V. D. Wal, R. V. Weeren, H. Weggemans, P. Weltevrede, S. White, S. J. Wijnholds, T. Wilhelmsson, O. Wucknitz, S. Yatawatta, P. Zarka, A. Zensus, and J. V. Zwieten, Astronomy Astrophysics **556**, A2 (2013).

[9] C. Sterpka, J. Dwyer, N. Liu, N. Demers, B. Hare, and O. Scholten, Uncharacteristically slow discharge process observed preceding lightning initiation (2022).